

## Original Research

# Pathophysiologic Basis of Contrast Enhancement in Breast Tumors

M.V. Knopp, MD,<sup>1\*</sup> E. Weiss,<sup>1</sup> H.P. Sinn, MD,<sup>2</sup> J. Mattern, MD,<sup>1</sup> H. Junkermann, MD,<sup>3</sup> J. Radeleff,<sup>1</sup> A. Magener, MD,<sup>2</sup> G. Brix, MD,<sup>1</sup> S. Delorme, MD,<sup>1</sup> I. Zuna, PhD,<sup>1</sup> and G. van Kaick, MD<sup>1</sup>

**While the diagnostic benefits of gadolinium (Gd)-chelate contrast agents are firmly established in magnetic resonance imaging (MRI) of tumors, the pathophysiologic basis of the enhancement observed and its histopathologic correlate remained vague. Tumor angiogenesis is fundamental for growth and metastasis and also of interest in new therapeutic concepts. By correlative analysis of a) histology; b) vascular density (CD31); and c) vascular permeability (vascular permeability factor/vascular endothelial growth factor [VPF/VEGF]), we found a) significantly ( $P < 0.001$ ) faster exchange rates in malignant compared with benign breast lesions; b) distinct differences in enhancement characteristics between the histologic types (invasive ductal carcinoma, invasive lobular carcinoma, and ductal carcinoma in situ); and c) dependence of enhancement kinetics on the VPF/VEGF expression. The pathophysiologic basis for the differences in contrast enhancement patterns of tumors detectable by MRI is mainly due to vascular permeability, which leads to more characteristic differences than vascular density. MRI is able to subclassify malignant breast tumors due to their different angiogenic properties. J. Magn. Reson. Imaging 1999; 10:260-266. © 1999 Wiley-Liss, Inc.**

**Index terms:** MR, mammography; pathophysiologic model; contrast enhancement; Gd-chelates

INTEREST IN NEOVASCULARIZATION for understanding the pathogenesis of malignant tumors, especially breast cancer, has recently increased. Current findings of the structural basis of tumor microvascular hyperpermeability suggest that the vesiculo-vacuolar organelles (VVOs) provide the major pathway for the extravasation of circulating macromolecules across endothelia (1). Characterization of neovascularization up to now has

been done only by in vitro immunohistochemical methods. Dynamic MRI with high temporal resolution permits noninvasive assessment of extravasation of extracellular paramagnetic contrast agents such as gadolinium (Gd)-chelates. Applying this technique to breast cancer lesions permits in vivo assessment of angiogenesis. Evaluation of its clinical importance in recent studies confirmed that angiogenesis is an independent prognostic factor in breast cancer (Fig. 1) (2-4). New antiangiogenic concepts for therapy of breast lesions are being introduced (5-8).

The histopathologic factors influencing contrast enhancement of Gd-chelates has remained undetermined up to now. Several attempts have been made to characterize such contrast enhancement with respect to vascular density, but discrepancies were noted indicating that factors other than vessel density influence contrast enhancement (9,10). Vascular permeability factor (VPF), also known as vascular endothelial growth factor (VEGF), is one of several multifunctional cytokines; it strongly increases microvascular leakage and directly stimulates endothelial cell division and migration. VEGF prepares the extracellular matrix for the formation of new vessels by increasing microvascular permeability to plasma proteins. VEGF therefore leads to neoangiogenesis. VEGF is expressed and secreted at high levels in physiologic processes such as wound healing, during the menstrual cycle, etc. in a strongly regulated manner, while uncontrolled expression is seen in many tumor cells (11-14).

We analyzed MRI contrast enhancement patterns and their relationship to tumor vascularity (CD31) and expression of VEGF in in vivo breast carcinoma.

## MATERIALS AND METHODS

### Patients

Twenty-seven patients were selected by weighted randomization from a group of prospectively studied patients (9) with undetermined breast lesions and histologic confirmation. Histologic classification revealed 10 invasive ductal carcinomas (IDC), 6 invasive lobular carcinomas (ILC), 4 ductal carcinomas in situ (DCIS), 5 fibroadenomas, 1 benign phylloides tumor, and 1 mastopathic nodule. The average age was 51 years (benign

<sup>1</sup>Department of Radiology, German Cancer Research Center, 69120 Heidelberg, Germany.

<sup>2</sup>Department of Pathology, University of Heidelberg, 69120 Heidelberg, Germany.

<sup>3</sup>Department of Gynecology and Obstetrics, University of Heidelberg, 69120 Heidelberg, Germany.

Contract grant sponsors: Tumorzentrum Heidelberg/Mannheim, Verein zur Förderung der Krebserkennung und Krebsbehandlung e.v., and ECR 97 fellowship.

\*Address reprint requests to: M.V.K., Department of Radiology, German Cancer Research Center, Im Neuenheimer Feld 280, 69120 Heidelberg, Germany. E-mail: m.knopp@dkfz-heidelberg.de

Received July 12, 1999; Accepted July 13, 1999.

© 1999 Wiley-Liss, Inc.

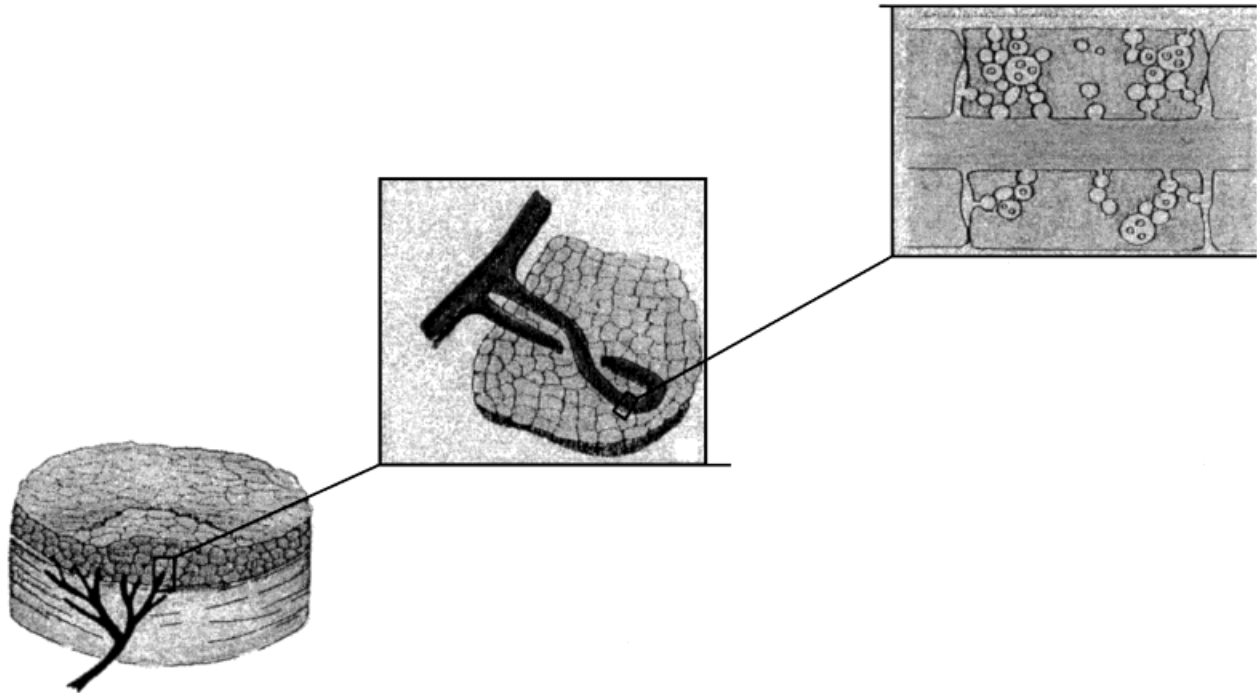


**Figure 1.** Sketch of pathophysiologic concept of neoangiogenesis. The induction of new vessel growth is the prerequisite for further tumor growth. Initially, the permeability of the surrounding tumor vasculature increases, which leads to extravasation of macromolecules. The increased permeability seems to be due to the vesiculo-vacuolar organelles. Their number and leakage is regulated by VEGF. The gadolinium-chelate contrast agents also use this route for extravasation, which leads to the more rapid and intense contrast enhancement in VEGF-activated tumor tissue.

lesions 41 and malignant 54 years). Patients were referred for functional magnetic resonance mammography (FMRM) from a breast clinic; all patients had a documented clinical history, X-ray mammography, and ultrasonography.

The MR mammographic exam included a static three-dimensional fast low-angle shot (3D-FLASH) pre- and post-contrast acquisition (TR/TE 20/5 msec,  $\alpha$  50°, field of view [FOV] 320 mm). For dynamic analysis, an optimized saturation recovery turbo-FLASH sequence with a temporal resolution of 1.3 seconds was used ( $T_{\text{REC}}$  125 msec, TE/TR 4/9 msec,  $\alpha$  12°). Fifteen parallel sections covering both breasts were acquired with a slice repetition time of 23 seconds. Gadolinium-diethylene triamine pentaacetic acid (DTPA) was used as paramagnetic contrast agent (Magnevist, Berlex, Wayne, NJ) and was infused by automated administration (CAI 626 P, Doltron, Uster, Switzerland) with a dose of 0.1 mmol/kg body weight within a constant time period of 60 seconds. All studies were performed using a standard 1.5 T clinical MRI system (Magnetom SP 4000, Siemens, Iselin, NJ). Patients were positioned prone with the breast freely hanging into the standard double-lumen breast coil. The total examination time was 25 minutes. Data analysis was done off-line on a VAX Alpha 3000/500 (DEC, Maynard, NJ) using a self-developed software.

Contrast enhancement was quantified using a previously described pharmacokinetic two-compartment model that quantifies the intensity of enhancement as the parameter amplitude (Amp [a.u.]), redistribution

rate constant ( $k_{21}$  [ $\text{min}^{-1}$ ]), and elimination rate constant ( $k_{e1}$  [ $\text{min}^{-1}$ ]) (15).

All lesions were surgically removed, and tumor tissue was fixed in buffered formalin for at least 24 hours and embedded in paraffin. The thickness of the tissue sections was approximately 2  $\mu\text{m}$ . The tissue sections were deparaffinized through storage for 24 hours in a pre-heated incubation case at 37°C; after storage at 50°C for another 30 minutes, the sections were put into xylene for  $2 \times 10$  minutes, followed by rehydration through a graded series of ethanol (100%, 96%, 70% each for 5 minutes). Before immunohistochemical staining, the tissue sections underwent a microwaving procedure after addition of a diluted antigen retrieval buffer (DAKO, Glostrup, Denmark) for 10 minutes at a high energy setting. After the addition of 50 ml of distilled  $\text{H}_2\text{O}$ , an additional 7 minutes of high microwave energy was applied. The slides were allowed to cool off at room temperature for a minimum of 20 minutes.

Sections were stained using an automated immunohistochemical technique (Biotek TechMate, Biotek Solutions, Newport Beach, CA) with strict adherence to the staining protocol. In brief, the primary antibodies are applied for 30 minutes, followed by an indirect streptavidin-biotin method with 30 minutes of secondary goat-anti-mouse antibody and 45 minutes of streptavidin biotin conjugate. Blood vessels were highlighted by staining endothelial cells for CD31 (DAKO, Hamburg, Germany; dilution 1:200). Microvessel density was determined in the area of most intense vascularization ("hot spot"). Individual counts were made on a 400 $\times$

Table 1

Overview of the Differences Between Benign and Malignant Lesions as Well as Between IDC and ILC (Pharmacokinetic Parameters and Vascular Density)

	Malignant (n = 20)	Benign (n = 7)	P value	IDC (n = 10)	ILC (n = 6)	P value
Amp (a.u.)	1.09 ± 0.62	1.73 ± 1.37	n.s.	1.33 ± 0.69	0.87 ± 0.45	n.s.
$k_{21}$ (min <sup>-1</sup> )	1.51 ± 1.04	0.56 ± 0.32	<0.001	1.86 ± 1.12	1.22 ± 0.9	n.s.
$k_{el}$ (min <sup>-1</sup> )	0.03 ± 0.04	0.03 ± 0.06	n.s.	0.05 ± 0.04	0.0 ± 0.03	<0.01
VD (CD31)	16 ± 6	13 ± 5	n.s.	15 ± 6	17 ± 7	n.s.

field (40× objective and 10× ocular, corresponding to an area of 0.152 mm<sup>2</sup>). Structures were only counted as microvessels if they stained positively with the vascular marker and morphologically appeared vascular, ie, had a lumen surrounded by endothelium. Staining for VEGF protein was performed using a commercially available polyclonal anti-VEGF<sub>165</sub> antibody (Dianova, Hamburg, Germany; dilution 1:10). For evaluation of VEGF expression, immunostains were graded as (-), (±), (+), and (++) depending on staining intensity. A tumor with grade (+) and (++) was classified as VEGF positive, and a tumor with (-) or (±) staining was regarded as VEGF negative.

Statistical significance of the quantitative data was determined by a Pearson correlation coefficient, regression analysis, and Student's *t*-test procedures calculated by SAS software (Gary, IN) and ROC analysis.

## RESULTS

### Contrast Enhancement Patterns in MRI

Detailed assessment of the enhancement patterns of the Gd-chelate contrast agent was allowed by the optimized saturation recovery turbo-FLASH sequence with high temporal resolution. Different contrast enhancement patterns were observed not only between benign and malignant histologies, but also depending on the histologic subentity.

Benign contrast-enhancing lesions presented a greater variability in intensity of enhancement, quantified by the pharmacokinetic parameter amplitude (A), than the malignant lesions (benign: mean A 1.73 ± 1.37 a.u.; malignant: mean A 1.09 ± 0.62 a.u.) (Table 1). The exchange rate of the contrast agent between the intra- and extravascular space, quantified by the pharmacokinetic parameter redistribution rate constant ( $k_{21}$ ), was found to be significantly lower ( $P < 0.001$ ) in benign lesions (mean  $k_{21}$  0.56 ± 0.32 min<sup>-1</sup>) than in malignant lesions (mean  $k_{21}$  1.51 ± 1.04 min<sup>-1</sup>). Analyzing only the malignant lesions, significantly ( $P < 0.01$ ) higher elimination rates ( $k_{el}$ ) were found in invasive ductal carcinomas (IDC) (mean  $k_{el}$  0.05 ± 0.04 min<sup>-1</sup>) than in invasive lobular carcinomas (ILC) (mean  $k_{el}$  0.00 ± 0.03 min<sup>-1</sup>) coinciding with lower amplitude (A) and exchange rate ( $k_{21}$ ) in ILC than IDC.

### Immunohistochemical CD31 and VEGF Staining

The vascular density (CD31) revealed no significant difference between the malignant and benign contrast-enhancing breast lesions (malignant: mean VD[CD31] 16 ± 6, benign: mean VD[CD31] 13 ± 5).

A basic VEGF stain was seen in the vascular and ductal endothelium in all lesions, as expected. Twelve of the 20 malignant breast lesions had a high VEGF expression (7 IDC, 4 ILC, 1 DCIS). Low VEGF expression was found in 8 malignant breast lesions (3 IDC, 2 ILC, and 3 DCIS). Analysis of the pharmacokinetic parameters in regard to VEGF expression revealed that significantly different ( $P < 0.005$ )  $k_{21}$  values were found between VEGF-positive and VEGF-negative tumors (mean  $k_{21}$  1.83 ± 1.03 min<sup>-1</sup> versus mean  $k_{21}$  0.74 ± 0.60 min<sup>-1</sup>) (Table 2). Values for amplitude (A) were higher in VEGF-positive lesions than in VEGF-negative lesions but not significantly. Vascular density (CD31) was significantly higher ( $P < 0.05$ ) in VEGF-positive than in VEGF-negative lesions (mean VD[CD31] 17 ± 6 versus mean VD[CD31] 13 ± 4). VEGF expression correlates by linear regression analysis most closely with the  $k_{21}$  value ( $r = 0.52$ ,  $P < 0.05$ ).

To analyze the relationship among VEGF,  $k_{21}$ , and CD31, the Pearson correlation coefficient was determined; no correlation was seen between  $k_{21}$  and CD31 in VEGF-positive lesions, whereas VEGF-negative lesions presented a correlation coefficient of  $r = 0.71$  ( $P < 0.07$ ).

Reviewing only the malignant lesions in regard to VEGF expression, significant differences are seen with a faster rate of enhancement in VEGF-positive lesions (mean  $k_{21}$  1.93 ± 1.03 min<sup>-1</sup> versus mean  $k_{21}$  0.88 ± 0.72 min<sup>-1</sup>; Table 3). This coincides with higher vascular density in VEGF-positive lesions. Limiting the analysis only to IDC and ILC, significantly higher intensity (Amp) and rate of enhancement ( $k_{21}$ ) are seen for VEGF-positive tumors.

## DISCUSSION

### In Vitro and In Vivo Description of Vascularization

The impact of neoangiogenesis, especially in breast cancer, has recently been demonstrated by in vitro analysis (16–18); in vivo patient studies are lacking. After implementing high temporal resolution imaging and pharmacokinetic analysis, we were able to assess

Table 2  
Comparison of Pharmacokinetic Parameters and Vascular Density (CD31) in Regard to VEGF Expression

	VEGF +	VEGF -	P value
Amp (a.U.)	1.37 ± 0.58	1.20 ± 1.04	n.s.
$k_{21}$ (min <sup>-1</sup> )	1.83 ± 1.04	0.74 ± 0.60	<0.005
$k_{el}$ (min <sup>-1</sup> )	0.037 ± 0.001	0.02 ± 0.06	n.s.
CD31	17 ± 6	13 ± 4	<0.05

Table 3

Comparison of Pharmacokinetic Parameters and Vascular Density (CD31) in Regard to VEGF Expression Within all Malignant Lesions and in the Combined IDC and ILC Subpopulation

	Malign			IDC and ILC		
	VEGF (+) (n = 12)	VEGF (-) (n = 8)	P value	VEGF (+) (n = 11)	VEGF (-) (n = 5)	P value
Amp	1.29 ± 0.53	0.87 ± 0.39	n.s.	1.33 ± 0.62	0.78 ± 0.42	<0.02
$k_{21}$ (min <sup>-1</sup> )	1.93 ± 1.02	0.88 ± 0.72	<0.01	2.05 ± 0.97	0.65 ± 0.45	<0.01
$k_{el}$ (min <sup>-1</sup> )	0.03 ± 0.03	0.03 ± 0.06	n.s.	0.03 ± 0.03	0.02 ± 0.06	n.s.
VD (CD31)	17 ± 6	14 ± 5	<0.05	18 ± 6	13 ± 4	n.s.

the enhancement pattern in tumors quantitatively, thus allowing comparison of the histologic and immunohistochemical parameters with in vivo MRI findings (Fig. 2). In this study the pharmacokinetic MRI properties are evaluated in respect to the in vivo vascularization of breast lesions; use of this technique for cervical cancer has been reported previously (19). Comparing IDC with ILC in MRI, IDC reveals a more rapid enhancement and elimination of the contrast agent than ILC. These distinctive enhancement patterns can only be explained by differences in vascularization (9,20).

From the pathologic point of view, IDC is more frequently associated with axillary node metastases and has a higher proliferative activity. ILC is characterized by diffuse infiltrative growth and a low propensity for lymphatic vessel invasion (21). These difference in biologic behavior seem to be associated with differences in angiogenesis. Dynamic MRI therefore mirrors the biologic and histologic properties of angiogenesis of breast tumors and can therefore be exploited for the differentiation of lesions into benign and malignant types. It may also potentially be a prognostic tool, especially in regard to metastasis and survival.

### Vascular Density and Vascular Hyperpermeability in MRI

We confirmed that the intensity of contrast enhancement in a lesion, which is a classic diagnostic criteria, is not the best feature to differentiate malignant and benign lesions. However, significant differences ( $P < 0.001$ ) were detected in regard to the pharmacokinetic exchange rate ( $k_{21}$ ) between benign and malignant breast tumors. In addition, the exchange rate shows significant differences ( $P < 0.005$ ) depending on expression of VEGF. Recent observations confirm that neoangiogenesis, which enables tumor growth, includes generation of new blood vessels as well as hyperpermeability (12,22–26). VEGF is one of the most potent known inducers of microvascular hyperpermeability. Several MRI studies have demonstrated that characteristic differences in contrast enhancement can be observed in breast lesions (27,28), but none demonstrated in vivo a correlation to VEGF expression.

Pearlman et al (29) reported that dynamic MRI can be used to identify and quantify non-invasively the benefits related to VEGF infusion on collateral vessel development in the ischemic myocardium of Yorkshire pigs. They concluded that MRI allows a non-invasive characterization of perfusion-related changes in different parts of the myocardium (30–33). We used a similar MRI technique in patients with breast cancer and analyzed

the perfusion characteristics in respect to VEGF expression and vascular density. As in a previous study (9), we were able to demonstrate that significant differences in the pharmacokinetic redistribution rate constant ( $k_{21}$ ) exist between benign and malignant breast lesions. Due to the small sample size ( $n = 27$ ), some differences in the pharmacokinetic parameters of the histologic entities are not significant (such as  $k_{21}$  between IDC and ILC), while they were significant in the larger study population ( $n = 314$ ), which did not employ immunohistochemical staining. The exchange rate  $k_{21}$  is the quantitative parameter that most closely correlates with VEGF expression. In tumors without elevated expression of VEGF, a linear correlation between  $k_{21}$  and microvessel density as reflected by CD31 was noted. Once the VEGF expression is elevated, the permeability assessed by  $k_{21}$  increases more rapidly and independently of microvessel density, leading to no further correlation.

### Pathophysiologic Basis of Contrast Enhancement

It has been accepted that differences in the angiogenesis of tumors are reflected by the different patterns of contrast enhancement in MRI, but the pathophysiologic basis has remained uncertain. Dvorak et al (1) compared the pattern of distribution of tracers with different molecular weights. Macromolecular tracers preferentially cross hyperpermeable tumor microvessels through VVOs (34,35). VVOs are grape-like clusters of interconnecting uncoated vesicles and vacuoles that span the entire thickness of vascular endothelium cells that line tumor, thereby providing a potential trans-endothelial connection between the vascular lumen and the extravascular space. The characteristic increase of permeability in tumor vessels is probably attributable to upregulation of VVO function. Qu-Hong et al (35) observed an intense immunostaining for VEGF on the abluminal plasma membrane of tumor-associated microvascular endothelial cells and in VVOs present in these same endothelial cells.

The pattern of distribution and extravasation of macromolecular tracers described by Dvorak et al (1) through VVOs coincides with the observed transit time by pharmacokinetic analysis in breast lesions. The VVOs might also be the most important pathway for the Gd-chelate MRI contrast agent. This indicates that dynamic MRI might be the preferential method for in vivo analysis of extravasation.

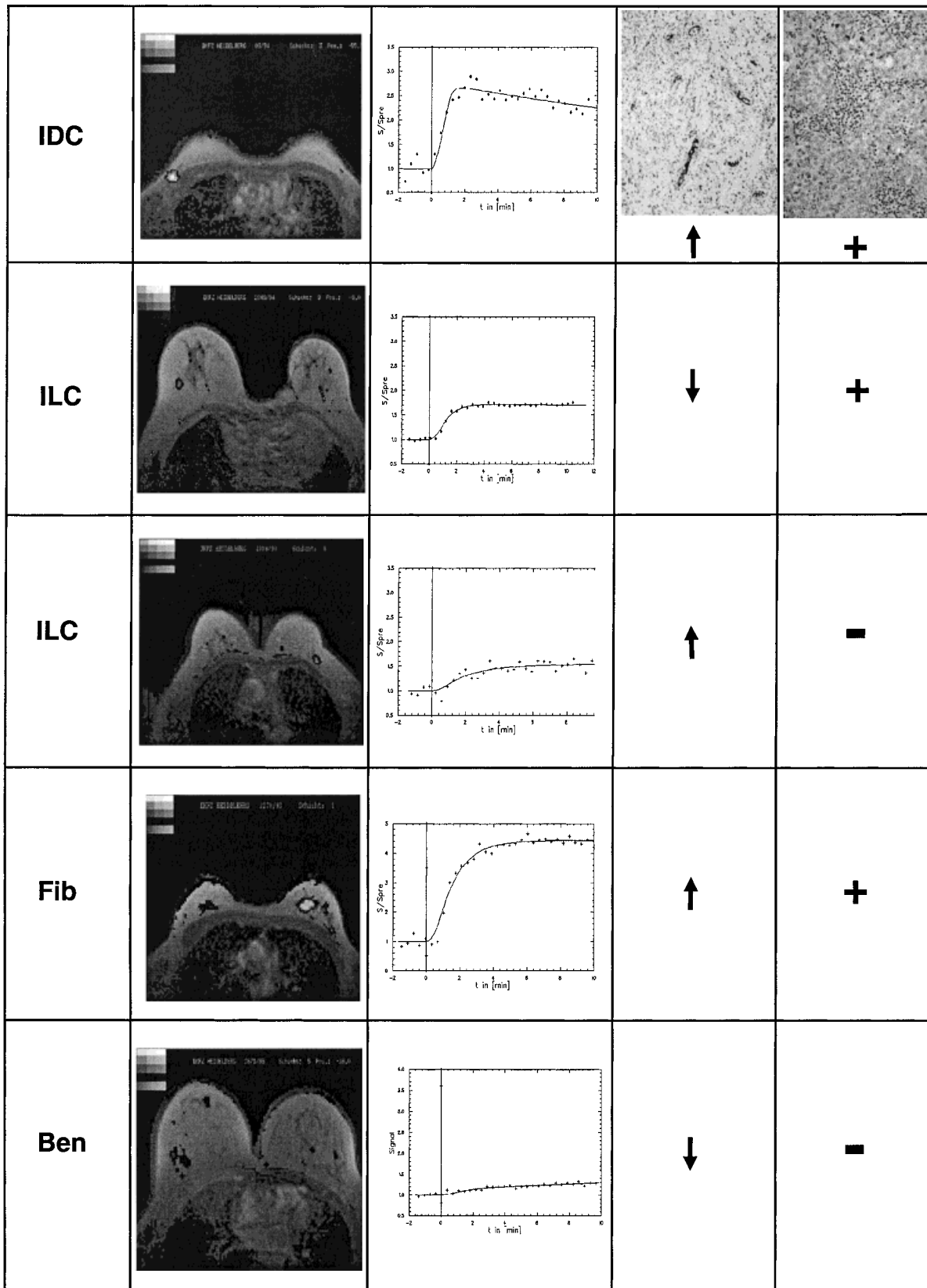


**Figure 2.** Overview of characteristic cases with fMRM color-coded enhancement images, time-intensity curves, and immunohistochemical findings for CD31 and VEGF. CD31 is used to identify the vascular density and VEGF the permeability. VEGF-positive tumors reveal a typical enhancement pattern with rapid increase to a maximum, whereas VEGF-negative tumors have a slower rate of enhancement. High vascular density leads to high amplitude of contrast enhancement. Column 1, histology; column 2, color-coded enhancement image; column 3, time-intensity curve; column 4, CD31 stain (↑ high, ↓ low); column 5, VEGF stain (+ positive stain – negative stain).

### **Clinical Impact of Vascular Density and Permeability**

The findings indicate that in vivo permeability seems to be a distinctive property whose clinical impact needs further assessment. Currently, in vitro studies are focused on vascular density (36–39). Weidner et al demonstrated a nearly linear relationship between microvessel counts in the areas of most vascularization (hot spots) and the metastatic potential of each tumor (2,25,40,41). Gasparini et al (42) also reported that intensity of angiogenesis is the strongest independent predictor of relapse-free survival in patients with node-negative breast cancer. Toi et al described a significant association between VEGF expression and microvessel count. Both were associated with relapse-free survival in univariate analysis (43,44).

### **Diagnostic and Therapeutic Implications**

Dynamic MRI mirrors biologic and histologic properties of angiogenesis of breast tumors and can be exploited for the differentiation of lesions into benign and malignant types and potentially as a prognostic tool especially in regard to lymphatic metastasis. It can therefore be postulated that MRI assessment may also provide a non-invasive prognostic indicator analogous to VEGF expression and microvessel count. A current application of MRI is already for assessment of changes in angiogenesis during neoadjuvant chemotherapy (45). Furthermore, MRI should be the modality most suited for non-invasive monitoring during anti-angiogenetic therapy (6,46–48).

### **ACKNOWLEDGMENTS**

M.V.K. received the ECR Research and Education Grant 97.

### **REFERENCES**

1. Dvorak AM, Kohn S, Morgan ES, et al. The vesiculo-vacuolar organelle (VVO): a distinct endothelial cell structure that provides a transcellular pathway for macromolecular extravasation. *J Leukoc Biol* 1996;59:100–115.
2. Craft PS, Harris AL. Clinical prognostic significance of tumour angiogenesis. *Ann Oncol* 1994;5:305–311.
3. Goulding H, Abdul Rashid NF, Robertson JF, et al. Assessment of angiogenesis in breast carcinoma: an important factor in prognosis? [see comments]. *Hum Pathol* 1995;26:1196–1200.
4. Weidner N, Folkman J, Pozza F, et al. Tumor angiogenesis: a new significant and independent prognostic indicator in early-stage breast carcinoma [see comments]. *J Natl Cancer Inst* 1992;84:1875–1887.
5. Harris AL, Zhang H, Moghaddam A, et al. Breast cancer angiogenesis—new approaches to therapy via antiangiogenesis, hypoxic activated drugs, and vascular targeting. *Breast Cancer Res Treat* 1996;38:97–108.
6. Hawkins MJ. Clinical trials of antiangiogenic agents. *Curr Opin Oncol* 1995;7:90–93.
7. Horak ER, Harris AL, Stuart N, Bicknell R. Angiogenesis in breast cancer. Regulation, prognostic aspects, and implications for novel treatment strategies. *Ann NY Acad Sci* 1993;698:71–84.
8. Marshall JL, Hawkins MJ. The clinical experience with antiangiogenic agents. *Breast Cancer Res Treat* 1995;36:253–261.
9. Knopp MV, Hoffmann U, Brix G, et al. Fast MRI contrast medium dynamics for characterization of tumors. Experiences with functional MR-mammography. *Radiology* 1995;35:964–972.
10. Furman HE, Margalit R, Grobgeld D, Degani H. Dynamic contrast-enhanced magnetic resonance imaging reveals stress-induced angiogenesis in MCF7 human breast tumors. *Proc Natl Acad Sci USA* 1996;93:6247–6251.
11. Folkman J. Tumor angiogenesis and tissue factor [comment]. *Nature Med* 1996;2:167–168.
12. Kolch W, Martiny Baron G, Kieser A, Marme D. Regulation of the expression of the VEGF/VPS and its receptors: role in tumor angiogenesis. *Breast Cancer Res Treat* 1995;36:139–155.
13. Senger DR, Brown LF, Claffey KP, Dvorak HF. Vascular permeability factor, tumor angiogenesis and stroma generation. *Invasion Metast* 1994;14:385–394.
14. Senger DR, van de Water L, Brown LF, et al. Vascular permeability factor (VPF, VEGF) in tumor biology. *Cancer Metast Rev* 1993;12:303–324.
15. Hoffmann U, Brix G, Knopp MV, Hess T, Lorenz WJ. Pharmacokinetic mapping of the breast: a new method for dynamic MR mammography. *Magn Reson Med* 1995;33:506–514.
16. Folkman J. Angiogenesis and breast cancer [editorial; comment]. *J Clin Oncol* 1994;12:441–443.
17. Gasparini G. Biological and clinical role of angiogenesis in breast cancer. *Breast Cancer Res Treat* 1995;36:103–107.
18. Weidner N. Angiogenesis in breast cancer. *Cancer Treat Res* 1996;83:265–301.
19. Hawighorst H, Knapstein PG, Weikel W, et al. Angiogenesis of uterine cervical carcinoma: characterization by pharmacokinetic magnetic resonance parameters and histological microvessel density with correlation to lymphatic involvement. *Cancer Res* 1997;57:4777–4786.
20. Brown LF, Berse B, Jackman RW, et al. Expression of vascular permeability factor (vascular endothelial growth factor) and its receptors in breast cancer. *Hum Pathol* 1995;26:86–91.
21. Sinn HP, Kellerhoff NM, Kellerhoff R, Bastert G, Otto HF. Subtyping and prognostic assessment of invasive lobular breast carcinoma. *Pathologe* 1997;18:37–44.
22. Connolly DT. Vascular permeability factor: a unique regulator of blood vessel function. *J Cell Biochem* 1991;47:219–223.
23. Dvorak HF, Detmar M, Claffey KP, et al. Vascular permeability factor/vascular endothelial growth factor: an important mediator of angiogenesis in malignancy and inflammation. *Int Arch Allergy Immunol* 1995;107:233–235.
24. Ferrara N. The role of vascular endothelial growth factor in pathological angiogenesis. *Breast Cancer Res Treat* 1995;36:127–137.
25. Fidler IJ, Ellis LM. The implications of angiogenesis for the biology and therapy of cancer metastasis [comment]. *Cell* 1994;79:185–188.
26. Senger DR. Molecular framework for angiogenesis: a complex web of interactions between extravasated plasma proteins and endothelial cell proteins induced by angiogenic cytokines [comment]. *Am J Pathol* 1996;149:1–7.
27. Fischer U, von HD, Vosschenrich R, Vieweg I, Grabbe E. Signal characteristics of malignant and benign lesions in dynamic 2D-MRT of the breast. *Rofo Fortschr Geb Rontgenstr Neuen Bildgeb Verfahr* 1993;158:287–292.
28. Gribbestad IS, Nilsen G, Fjosne H, et al. Contrast-enhanced magnetic resonance imaging of the breast. *Acta Oncol* 1992;31:833–842.
29. Pearlman JD, Hibberd MG, Chuang ML, et al. Magnetic resonance mapping demonstrates benefits of VEGF-induced myocardial angiogenesis. *Nature Med* 1995;1:1085–1089.
30. Brasch RC, Schwicker HC, Roberts TP, et al. Definition of peritumoral vessels with contrast-enhanced magnetic resonance imaging: comparison of gadopentetate dimeglumine and a blood-pool macromolecular contrast medium. *Acad Radiol* 1996;3(suppl 2):S347–348.
31. Brasch RC, Shames DM, Cohen FM, et al. Quantification of capillary permeability to macromolecular magnetic resonance imaging contrast media in experimental mammary adenocarcinomas. *Invest Radiol* 1994;29(suppl 2):S8–11.
32. Cohen FM, Kuwatsuru R, Shames DM, et al. Contrast-enhanced magnetic resonance imaging estimation of altered capillary permeability in experimental mammary carcinomas after X-irradiation. *Invest Radiol* 1994;29:970–977.

33. van Dijke CF, Brasch RC, Roberts TP, et al. Mammary carcinoma model: correlation of macromolecular contrast-enhanced MR imaging characterizations of tumor microvasculature and histologic capillary density. *Acad Radiol* 1996;198:813-818.
34. Feng D, Nagy JA, Hipp J, Dvorak HF, Dvorak AM. Vesiculo-vacuolar organelles and the regulation of venule permeability to macromolecules by vascular permeability factor, histamine, and serotonin. *J Exp Med* 1996;183:1981-1986.
35. Qu Hong, Nagy JA, Senger DR, Dvorak HF, Dvorak AM. Ultrastructural localization of vascular permeability factor/vascular endothelial growth factor (VPF/VEGF) to the abluminal plasma membrane and vesiculovacuolar organelles of tumor microvascular endothelium. *J Histochem Cytochem* 1995;43:381-389.
36. Bosari S, Lee AK, DeLellis RA, et al. Microvessel quantitation and prognosis in invasive breast carcinoma. *Hum Pathol* 1992;23:755-761.
37. Guidi AJ, Fischer L, Harris JR, Schnitt SJ. Microvessel density and distribution in ductal carcinoma in situ of the breast. *J Natl Cancer Inst* 1994;86:614-619.
38. Vartanian RK, Weidner N. Correlation of intratumoral endothelial cell proliferation with microvessel density (tumor angiogenesis) and tumor cell proliferation in breast carcinoma. *Am J Pathol* 1994;144:1188-1194.
39. Zhang HT, Craft P, Scott PA, et al. Enhancement of tumor growth and vascular density by transfection of vascular endothelial cell growth factor into MCF-7 human breast carcinoma cells. *J Natl Cancer Inst* 1995;87:213-219.
40. Toi M, Kashitani J, Tominaga T. Tumor angiogenesis is an independent prognostic indicator in primary breast carcinoma. *Int J Cancer* 1993;55:371-374.
41. Weidner N, Semple JP, Welch WR, Folkman J. Tumor angiogenesis and metastasis—correlation in invasive breast carcinoma. *N Engl J Med* 1991;324:1-8.
42. Gasparini G, Harris AL. Clinical importance of the determination of tumor angiogenesis in breast carcinoma: much more than a new prognostic tool. *J Clin Oncol* 1995;13:765-782.
43. Toi M, Inada K, Suzuki H, Tominaga T. Tumor angiogenesis in breast cancer: its importance as a prognostic indicator and the association with vascular endothelial growth factor expression. *Breast Cancer Res Treat* 1995;36:193-204.
44. Toi M, Hoshina S, Takayanagi T, Tominaga T. Association of vascular endothelial growth factor expression with tumor angiogenesis and with early relapse in primary breast cancer. *Jpn J Cancer Res* 1994;85:1045-1049.
45. Knopp MV, Brix G, Junkermann HJ, Sinn HP. MR mammography with pharmacokinetic mapping for monitoring of breast cancer treatment during neoadjuvant therapy. *Magn Reson Imaging Clin North Am* 1994;2:633-658.
46. Kim KJ, Li B, Winer J, et al. Inhibition of vascular endothelial growth factor-induced angiogenesis suppresses tumour growth in vivo. *Nature* 1993;362:841-844.
47. Sioussat TM, Dvorak HF, Brock TA, Senger DR. Inhibition of vascular permeability factor (vascular endothelial growth factor) with antipeptide antibodies. *Arch Biochem Biophys* 1993;301:15-20.
48. Weidner N, Borgstrom P, Hillan KJ, et al. Complete inhibition of angiogenesis and growth of microtumors by anti-vascular endothelial growth factor neutralizing antibody: novel concepts of angiostatic therapy from intravital videomicroscopy. *Breast Cancer Res Treat* 1991;47:211-218.